Since January 2020 Elsevier has created a COVID-19 resource centre with free information in English and Mandarin on the novel coronavirus COVID-19. The COVID-19 resource centre is hosted on Elsevier Connect, the company's public news and information website.

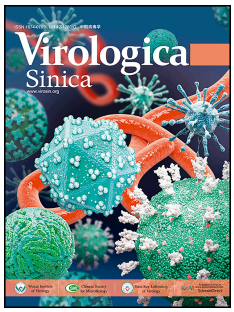

Quantitative determination of the electron beam radiation dose for SARS-CoV-2 inactivation to decontaminate frozen food packaging

Zihao Wang, Zhentao Liang, Rongguo Wei, Hongwei Wang, Fang Cheng, Yang Liu, Songdong Meng

PII: S1995-820X(22)00182-1

DOI: https://doi.org/10.1016/j.virs.2022.10.007

Reference: VIRS 123

To appear in: *Virologica Sinica*

Received Date: 1 July 2022

Accepted Date: 21 October 2022

Please cite this article as: Wang, Z., Liang, Z., Wei, R., Wang, H., Cheng, F., Liu, Y., Meng, S., Quantitative determination of the electron beam radiation dose for SARS-CoV-2 inactivation to decontaminate frozen food packaging, *Virologica Sinica*, https://doi.org/10.1016/j.virs.2022.10.007.

VS6040

Research Article

Received: 1 July 2022, Accepted: 21 October 2022

Quantitative determination of the electron beam radiation dose for SARS-CoV-2 inactivation to decontaminate frozen food packaging

Zihao Wang[1,2,#], Zhentao Liang[1,2,#], Rongguo Wei[1,2,3,#], Hongwei Wang[4], Fang Cheng[1,2], Yang Liu[5], Songdong Meng,[1*]

[1] Key Laboratory of Pathogenic Microbiology and Immunology, Institute of Microbiology, Chinese Academy of Sciences, Beijing 100101, China

[2] University of Chinese Academy of Sciences, Beijing 100049, China

[3] Department of Clinical Laboratory, the Fifth Affiliated Hospital of Guangxi Medical University, Nanning 530022, China

[4] China Isotope and Radiaton Corporation, Beijing 100089, China

[5] Changchun CNNC CIRC Radiation Technology Co., LTD, Jilin 130022, China

* Corresponding author.

E-mail addresses: mengsd@im.ac.cn

ORCID: https://orcid.org/0000-0001-5670-1533

[#] Zihao Wang, Zhentao Liang, and Rongguo Wei contributed equally to this work.

Highlights

Electron beam irradiation is an effective approach for SARS-CoV-2 inactivation under cold-chain conditions.
The effective inactivation dose was defined as 3 kGy that is far below the safe limit for food processing.
Cell-based virus assays are essential to evaluate the SARS-CoV-2 inactivation efficiency for the decontaminating strategies.

Abstract:

The spread of severe acute respiratory syndrome coronavirus 2 (SARS-CoV-2) from cold-chain foods to frontline workers poses a serious public health threat during the current global pandemic. There is an urgent need to design concise approaches for effective virus inactivation under different physicochemical conditions to reduce the risk of contagion through viral contaminated surfaces of cold-chain foods. By employing a time course of electron beam exposure to a high titer of SARS-CoV-2 at cold-chain temperatures, a radiation dose of 2 kGy was demonstrated to reduce the viral titer from $10^{4.5}$ to 0 $TCID_{50}$/mL. Next, using human coronavirus OC43 (HCoV-OC43) as a suitable SARS-CoV-2 surrogate, 3 kGy of high-energy electron radiation was defined as the inactivation dose for a titer reduction of more than 4 log units on tested packaging materials. Furthermore, quantitative reverse transcription PCR (RT-qPCR) was used to test three viral genes, namely, *E*, *N*, and *ORF1ab*. There was a strong correlation between median tissue culture infectious dose ($TCID_{50}$) and RT-qPCR for SARS-CoV-2 detection. However, RT-qPCR could not differentiate between the infectivity of the radiation-inactivated and nonirradiated control viruses. As the defined radiation dose for effective viral inactivation fell far below the upper safe dose limit for food processing, our results provide a basis for designing radiation-based approaches for the decontamination of SARS-CoV-2 in frozen food products. We further demonstrate that cell-based virus assays are essential to evaluate the SARS-CoV-2 inactivation efficiency for the decontaminating strategies.

Keywords: Severe acute respiratory syndrome coronavirus 2 (SARS-CoV-2); inactivation; electron beam radiation; food decontamination; cold-chain

1. Introduction

The coronavirus disease 2019 (COVID-19), which is caused by the severe acute respiratory syndrome coronavirus 2 (SARS-CoV-2), has resulted in a global health crisis and enormous social and economic distress (Wang et al., 2020). Previous studies have reported that SARS-CoV-2 is transmitted between humans, mainly via respiratory droplets or aerosol particles (Jarvis, 2020; W. Liu et al., 2020). However, cold-chain practitioners might be infected via contact with contaminated cold-chain foods that tested nucleic acid positive for SARS-CoV-2 (P. Liu et al., 2020). SARS-CoV-2 was detected up to 72 h after applying it to plastic and stainless steel at 21°C–23°C (van Doremalen N et al., 2020). At 4°C and −20°C, the virus on food surfaces remained infectious even after 21 days (Feng et al., 2021; Fisher, 2020). The Chinese Center for Disease Control and Prevention reported that the spread of SARS-CoV-2 from cold-chain foods to humans was likely one of the transmission routes of COVID-19 (Ma et al., 2021). All these studies raised concerns about the possible transmission of SARS-CoV-2 to humans via frozen food packages (Chen et al., 2022; Chi et al., 2021a, 2021b). Therefore, how to interrupt the potential cold-chain transmission of SARS-CoV-2 has become a global challenge.

Owing to its rapid spread and long survival time, it is critical to design effective disinfection approaches to cut off the viral transmission route. Currently, the commonly used disinfectants include ethanol, sodium hypochlorite, and ultraviolet radiation, which have shown remarkable inactivation efficiency against SARS-CoV-2 (Kampf et al., 2020; Leslie et al., 2021; Sellera et al., 2021). In addition to their potential toxic contamination of frozen food, chemical disinfectants tend to freeze in cold-chain environments, resulting in an obvious reduction in their disinfection efficiency. In contrast, ultraviolet radiation cannot penetrate the surfaces of food packaging materials, thereby leaving blind areas for virus inactivation (He et al., 2022; Ruetalo et al., 2021). Hence, it is urgent to explore efficient disinfection approaches to prevent cold-chain transmission. Irradiation with high-energy gamma rays or electron beams has long been used for sterilization of food and presents unique merits over other sterilization methods, including high penetrating power, environmental friendliness, and low harmful effects on the nutritional value of foods (Mousavi Khaneghah et al., 2020; Pillai SD and Shayanfar, 2017). However, employing irradiation techniques for the inactivation of SARS-CoV-2 has not been explored.

The purpose of this study was to determine the feasibility of using the irradiation approach for complete inactivation of SARS-CoV-2 on food packages under cold-chain conditions. The results will help to design strategies and tactics for the decontamination of frozen food products to reduce possible viral fomite transmission among frontline workers and customers.

2. Materials and Methods

2.1. Cell lines and viruses

Vero E6 (ATCC, CRL-1586) and BHK-21 (ATCC, CCL-10) cells were cultured in Dulbecco's modified eagle medium (DMEM) (HyClone, South Logan, UT, USA) supplemented with 10% fetal bovine serum (Gibco, Carlsbad, CA, USA), 100 IU/mL of penicillin, and 100 μg/mL of streptomycin.

SARS-CoV-2 (hCoV-19/China/CAS-B001/2020, National Microbiology Data Center NMDCN0000102-3, GISAID No. EPI_ISL_514256-7) and HCoV-OC43 (VR-1558) were obtained from the CAS Key Laboratory of Pathogenic Microbiology and Immunology, Institute of Microbiology, Chinese Academy of Sciences (CAS). The viral concentrations of two coronaviruses SARS-CoV-2 and HCoV-OC43 used in the study were the achievable stock concentrations, which are higher than the viral titers present in general clinical respiratory samples (1×10^3 to 1×10^4 $TCID_{50}$/mL) and meet the requirement (viral titer $\geq$ 4.0 logs) of the health industry standards of the People's Republic of China (WS/T 775-2021) (Pan et al., 2020; To KK et al., 2020; Zhang et al., 2021).

2.2. Virus inactivation with low-energy electron irradiation

Low-energy electron irradiation (LEEI) was performed with a 160 keV electron accelerator (MEB160 desktop electron beam equipment, Sichuan Zhiyan Technology Co., Ltd., Sichuan, China). All experiments based on SARS-CoV-2 were performed under biosafety level 3 (BSL-3). The SARS-CoV-2 and HCoV-OC43 stocks were serially diluted in DMEM without serum or BSA. Ten microliters of various concentrations of viral stocks were placed on stainless steel (12 mm diameters sterile disks) laid on 24-well plates under different temperature conditions (4 °C and −20 °C) until the sample surface was completely dry. The samples were treated with radiation doses of 0, 1.0, 2.0, 3.0, 6.0, and 9.0 kGy using LEEI according to the manufacturer's instruction (Fig. 1A). As the radiation source emitted the electron beam at a uniform rate, the exposure time was determined by set irradiation dose. Then the stainless steel was transferred to 1.5 mL microfuge tubes to extract virus based on the testing method ISO 18184:2019 (Textiles-Determination of antiviral activity of textile products). Briefly, 1 mL of serum-free DMEM was added in the containers, and then they were agitated by vortex mixer for 5 s and 5 times to wash out the virus from the specimens. Eluted virus samples were tested in duplicates using the $TCID_{50}$ assay to determine the radiation dose required for the complete inactivation of virus.

2.3. Virus recovery and $TCID_{50}$ assay

The median tissue culture infectious dose ($TCID_{50}$) assay was used to determine virus titration and performed in a 96-well plate with 4×10^4 cells/well. The cells were washed with PBS twice before inoculation of samples. The inactivated viral sampleswere serially diluted in DMEM without serum. The cells were incubated for 72 h at 37 °C with 5% CO_2. Cytopathic effects were recorded for the calculation of $TCID_{50}$ according to the Reed and Muench method.

2.4. Virus inactivation with high-energy electron irradiation

High-energy electron irradiation (HEEI) was performed with a 10 MeV electron accelerator (China Institute of Atomic Energy). The HCoV-OC43 stocks were serially diluted in DMEM without serum or BSA. Ten microliters of HCoV-OC43 viral stocks were placed on a stainless steel sheet (12 mm diameters sterile disks), filter paper (a square 10 mm on a side), and plastic (a square 10 mm on a side) in sealed microfuge tubes that were surface decontaminated with sodium hypochlorite, and the samples were kept at 4 °C or −20 °C. The samples were treated with radiation doses of 0, 1.0, 2.0, 3.0, and 6.0 kGy using HEEI according to the manufacturer's instructions (Fig. 1B). Viruses on different materials were resuspended completely in serum-

free DMEM based on the testing method ISO 18184:2019, and then the $TCID_{50}$ assay was used to determine the radiation dose required for the complete inactivation of the virus.

2.5. Extraction and quantification of viral RNA

Viral RNA was extracted from the cell supernatants as previously described (Näslund et al., 2008). Briefly, RNA was extracted and purified in 1.5 mL microfuge tubes using TRIzol™ LS reagent (Thermo Fisher, Waltham, MA, USA) and RNeasy Mini Kit (Qiagen Inc.) in accordance with the manufacturer's instructions. cDNA was synthesized using One Step PrimeScript III RT-qPCR Mix with UNG (Takara Bio, Shiga, Japan) according to the manufacturer's protocols. The primers and probes used are described in Supplementary Table S1. The PCR target region of *ORF1ab* gene was 100 bp, accounting for 0.470% of the total 21290 bp of *ORF1ab* gene. The PCR target region of *E* gene was 113 bp, accounting for 49.6% of the total 228 bp of the gene. The PCR target region of *N* gene was 128 bp, accounting for 10.2% of the total length of the gene 1260 bp. A total of 341 bp in length was targeted by PCR of the three genes, accounting for 1.14% of the total 29903 bp of the viral genome. Viral load was quantified using the cycle quantification (Cq) values.

2.6. Statistical analysis

All infection experiments were repeated in three independent experiments. Data analysis was performed in Microsoft Excel and GraphPad Prism (GraphPad Software, USA). The *t*-test was used to analyze the collected data and for all *P*-values, $P < 0.05$ was considered significant. R squared (R^2) values and *P*-values were calculated and used to determine the relationship between the Cq values and viral titers using simple linear regression and correlation analysis tools from GraphPad Prism.

3. Results

3.1. Determination of the minimal dose of LEEI for the complete inactivation of SARS-CoV-2 and HCoV-OC43

To test the viral inactivation ability of electron beam radiation, a time course of electron beam exposure was employed to determine the minimal amount of radiation required to inactivate SARS-CoV-2, as well as HCoV-OC43 as a SARS-CoV-2 surrogate, on the surface of stainless steel sheets that maintain the longest viability of SARS-CoV-2 (van Doremalen N et al., 2020). The LEEI was chosen due to the size limits of the electron accelerator in biosafety level 3 (BSL-3) laboratories. LEEI against $10^{4.6}$ median tissue culture infectious dose ($TCID_{50}$)/mL of SARS-CoV-2 suspensions completely inactivated viral infectivity in the presence of a radiation dose of 2.0, 3.0, 6.0, or 9.0 kGy at a temperature of 4°C or −20°C (Fig. 2A). Similar results were obtained for $10^{4.75}$ $TCID_{50}$/mL of HCoV-OC43 suspensions under the same conditions (Fig. 2B).

The viral inactivation efficiency of irradiation was determined using three cycles of infections. The Vero E6 monolayers infected with $10^{4.6}$ $TCID_{50}$/mL of SARS-CoV-2 after irradiation at doses of ≥ 2 kGy were fully protected (Fig. 2C). No cytopathic effect was observed when BHK-21 monolayers were infected with $10^{4.75}$ $TCID_{50}$/mL of HCoV-OC43 irradiated with a dose of 2 kGy or above (Fig. 2D). The experiments were conducted using the second and third passages of cell culture supernatants on corresponding cells, and the

cytopathic effect was monitored. A minimal dose of 2.0 kGy of LEEI caused more than a 99.99% reduction in SARS-CoV-2 titer, representing effective virucidal activity. Furthermore, the results indicate that HCoV-OC43 with moderate pathogenic potential to humans, has the same susceptibility to LEEI as that of SARS-CoV-2, and it can be used as a suitable surrogate for the highly pathogenic SARS-CoV-2.

3.2. Viral inactivation efficiency of HEEI on different packaging materials

The similar inactivation effect of radiation on SARS-CoV-2 and HCoV-OC43 demonstrates that HCoV-OC43 is a suitable candidate for surrogates for SARS-CoV-2. Hence, HCoV-OC43 was used for radiation inactivation tests in subsequent studies to avoid the potential infection risk of the experiment operators through aerosol particles during the extraction of SARS-CoV-2 from packaging materials. Plastic and filter paper were chosen to mimic cold-chain food packaging materials. HEEI was used because of its much better ability to penetrate the inner parts of the irradiated materials. As seen in Fig. 3A, the minimum effective inactivation dose, using HEEI, for $10^{4.5}$ $TCID_{50}$/mL of HCoV-OC43 suspension on stainless steel was 2 kGy at 4°C, which was identical to the inactivation dose when using LEEI. Unlike stainless steel, the minimum inactivation dose for HCoV-OC43 on plastic and filter paper was 3 kGy, indicating that HCoV-OC43 on these materials was more resistant to radiation. Similar results were observed at −20°C. Taken together, 3 kGy was determined as the minimum effective inactivation dose for a SARS-CoV-2 titer reduction of more than 4 log units on the surface of the tested materials.

3.3. Effect of radiation on SARS-CoV-2 detection using quantitative reverse transcription PCR (RT-qPCR) assay

Currently, the detection of SARS-CoV-2 on cold-chain food packaging surfaces is performed using viral RNA-based RT-qPCR methods (Feng et al., 2021; Guo et al., 2022; Li et al., 2022); hence, the effect of LEEI on the integrity and detectability of viral RNA was determined. The irradiated or nonirradiated viral suspensions were further assessed using RT-qPCR to measure the copy numbers of three viral genes, namely, envelope (*E*) (Fig. 4A), nucleocapsid (*N*) (Fig. 4B), and RNA-dependent RNA polymerase (*ORF1ab*) (Fig. 4C). Although irradiation at a 2.0-kGy dose inactivated viable SARS-CoV-2 to undetectable levels using the $TCID_{50}$ assay (Fig. 2), the respective quantitation cycle (Cq) values of these three viral genes scarcely changed after irradiation compared with that of the nonirradiated control ($P > 0.05$). This indicates that the radiation-treated viral RNA was unacted at least within the short PCR target regions of the *E*, *N*, and *ORF1ab* genes. The detection limit for the RT-qPCR-based assay for SARS-CoV-2 under irradiation was approximately $10^{3.5}$ $TCID_{50}$/mL if Cq values set within 30–35 cycles were valid.

Results of the viral *E* gene detection in viral suspensions irradiated with a 2-kGy dose showed that SARS-CoV-2 suspensions at $TCID_{50}$/mL of $10^{5.5}$ (Cq = 17.21), $10^{4.5}$ (Cq = 24.42), and $10^{3.5}$ (Cq = 27.44) fell within the linear range of the assay ($R^2 = 0.9056$) (Fig. 4D). Similar results were observed for the detection of the viral *N* (Fig. 4E) and *ORF1ab* (Fig. 4F) genes. These data show that there was a strong correlation between $TCID_{50}$ and RT-qPCR for the detection of SARS-CoV-2 on experimental fomites.

3.4. The combination of virus culture and RT-qPCR is feasible to evaluate the SARS-CoV-2 inactivation

efficiency

Since direct RT-qPCR could almost equally detect viable and radiation-inactivated SARS-CoV-2 on stainless steel, a combination of virus culture and RT-qPCR-based approach were explored to selectively test viable viruses. Neat and 10-fold dilutions of SARS-CoV-2 suspensions on stainless steel were collected and transferred to the Vero E6 cell culture. After 72 hours incubation, three viral genes in the supernatants of the infected cells were detected by RT-qPCR (Fig. 5A). The viruses in the supernatants of the Vero E6 cells incubated with untreated viral suspensions can be detected by RT-qPCR. In contrast, the RT-qPCR tests showed negative results in the supernatants of the Vero E6 cells incubated with radiation-inactivated viral suspensions. Further analysis showed that the RT-qPCR Cq values of the *E* gene were highly correlated with viral titers in the range of $10^{4.5}$–$10^{-0.5}$ $TCID_{50}$/mL (R^2 = 0.9351) (Fig. 5B). For the viral *N* gene, a correlation was observed between the Cq values and the $TCID_{50}$/mL titer from $10^{4.5}$–$10^{-1.5}$ (R^2 = 0.8703) (Fig. 5C). For the *ORF1ab* gene, the Cq values and $TCID_{50}$/mL titer from $10^{4.5}$–$10^{0.5}$ showed a linear relationship (R^2 = 0.8905) (Fig. 5D). These results validate the combination of virus culture and RT-PCR as a feasible approach to evaluate the SARS-CoV-2 inactivation efficiency for the decontaminating strategies.

4. Discussion

The current global SARS-CoV-2 pandemic is of urgent concern because of its high transmission rate, viral fast-growing mutations, vaccine escape, and spread throughout the world. Although vaccines and measures of infection prevention and control are available currently, infections are often reported in high-risk groups working in zones with high traffic of international cargo, such as borders, customs checkpoints, and airports (Peña et al., 2020; Widera et al., 2021). Thus, there is an urgent need to design concise approaches for effective virus inactivation under different physicochemical conditions, to reduce the risk of contagion through viral contaminated surfaces during the delivery of letters or freights (Ulloa et al., 2021). Most chemical biocides, such as electrolyzed water, ethanol, and sodium hypochlorite, demonstrate prompt anti-SARS-CoV-2 activity (Leslie et al., 2021; Takeda et al., 2020); however, their use is limited in foodstuff and organic substances, and their virucidal effects require certain conditions (Uema et al., 2021). Ultraviolet-C light irradiation is considered the most effective germicidal method that is adopted to inactivate various pathogenic species, but it has very limited penetration of packaging materials and the inner packing material (Inagaki et al., 2020; Ruetalo et al., 2021). Gamma radiation has been used to inactivate many types of microorganisms since 1971, though the method has certain logistical and technical limitations that may have substantial adverse effects on materials and humans (Al-Hadyan et al., 2021). Electron beam irradiation is another promising sterilization option. Previous studies have analyzed the sensitivity of various viruses and bacteria to HEEI (Brahmakshatriya et al., 2009; Jeong et al., 2021; Praveen et al., 2013; Preuss et al., 1997; Smolko and Lombardo, 2005). The viral inactivation efficiency of electrons is mainly dependent on doses irradiated, regardless of whether low- or high-energy electrons are used (Predmore et al., 2015).

In this study, we validated the virucidal activity of electron beam radiation and first defined the minimum

effective inactivation dose for a SARS-CoV-2 titer reduction of more than 4 log units under cold-chain temperatures (4°C and −20°C). HCoV-OC43 was selected as a suitable candidate for surrogates for the highly pathogenic SARS-CoV-2 because its sensitivity to radiation shared significant similarities with SARS-CoV-2 (Boegel et al., 2021; Song et al., 2019). At a dose of 2.0 kGy, LEEI reduced SARS-CoV-2 titer by more than 4 log units (99.99% reduction). Both LEEI (160 keV) and HEEI (10 MeV) inactivated HCoV-OC43 on stainless-steel surfaces with the same dose as that used for SARS-CoV-2. Food packaging materials, including plastic and filter paper, seem to be more refractory to radiation; therefore, the virus requires a higher dose (3 kGy) of HEEI to reduce the viral titer by 99.99% (Gidari et al., 2021). This may be partly because these organic materials scavenge the reactive species produced in the radiation matrix, which is known to reduce radiation effectiveness during treatment (Sommer et al., 2001).

To our knowledge, the effect of low-dose rate electron beam radiation on SARS-CoV-2 or other coronavirus activity has not been investigated. The indicator of the energy required to reduce a titer by one log (D_{10} value) is often used to evaluate the susceptibility of a virus to a sterilization method (Jain et al., 2021; Loveday et al., 2021). We could not calculate the D_{10} value (irradiation dose required to reduce 90% of the virus titer) because of the limitations of the irradiation machine and viral titer. The D_{10} value is calculated using the inverse of the slopes of the regression lines (1/slope) of irradiation dose against log virus titer (Jain et al., 2021). As seen in Fig.2A, $10^{4.6}$ $TCID_{50}$/mL of SARS-CoV-2 was the achievable stock concentration, and the virus at this titer was completely inactivated at a radiation dose of 2.0 kGy. For the irradiation machine we used in BSL-3 only integer dose values can be set, so we can only use two doses at most (0 and 1 kGy), which did not permit to draw the regression lines. Nevertheless, our results indicate a high effectiveness of electron beam radiation in inactivating SARS-CoV-2 and HCoV-OC43.

Food irradiation has long been used as a safe food processing technology for disinfection and prolonging shelf life. A joint committee formed by the Food and Agriculture Organization, International Atomic Energy Agency, and World Health Organization once concluded that food exposed to an ionizing radiation of less than 10 kGy did not cause any toxicological hazard, nutritional, or microbial problem (Diehl, 2002; Ravindran and Jaiswal, 2019). In our current study, 3 kGy was defined as the minimum radiation dose required for the nearly complete inactivation of SARS-CoV-2 in food packaging materials at cold-chain temperatures, which is far below the upper safe limit of 10 kGy for food processing. Therefore, our results will provide the basic key data for designing radiation-based approaches for decontamination of SARS-CoV-2 from frozen food products.

Electron beam radiation and gamma radiation are ionizing radiation. Their mechanisms of virus inactivation are thought to lead to disruption of the genetic material and protein/collagen damage (Dziedzic-Goclawska et al., 2005; Grieb et al., 2002; Ohshima et al., 1996; Summers and Szybalski, 1967; Ward RL., 1980). Radiation damage to nucleic acids of viruses is believed to play a major role in virucidal activity, whereas the minor molecular targets of the mechanisms are believed to be proteins and lipids in the viral envelope (Elliott et al., 1982; Hume et al., 2016; Korystov Yu N, 1992). The genome of SARS-CoV-2 is a positive-sense single-stranded RNA of 29.9 kb in length that contains 14 functional open reading frames encoding 29 structural,

nonstructural, and accessory proteins (Bai et al., 2022). The total PCR target regions of the *E*, *N*, and *ORF1ab* genes in the RT-qPCR assay account for approximately 1.14% of the total viral genome in length, which means that the most commonly used RT-qPCR method could very likely yield similar results regardless of whether the radiation damaged or intact viral genome is used. This was validated in our results that the Cq values of these three viral genes after 2 kGy lethal irradiation were not significantly different from those of the nonirradiated control group. A previous study showed that a 50-kGy dose of radiation was needed to accomplish complete viral RNA degradation and genes could not be detected using an RT-qPCR assay (Al-Hadyan et al., 2021). As the irradiation doses of 2–3 kGy may only cause minor damage to the viral genome, the irradiation-damaged viral genome could be easily detected by RT-qPCR in our current experiments. Our results therefore indicate that RT-qPCR-based detection is not suitable as the only method for evaluating the SARS-CoV-2 inactivation efficiency of radiation. Importantly, we further demonstrated that real-time PCR could only detect viral genes when applied to supernatants of Vero E6 cells harvested upon infection with SARS-CoV-2 untreated rather than treated with 2 kGy of radiation (Fig. 5), suggesting a combination of virus culture and RT-PCR as a feasible approach for evaluation of the SARS-CoV-2 inactivation efficiency. Taken together, we validate the biological assay of infectivity of viruses, including $TCID_{50}$ assays, rather than RT-qPCR methods, which is mandatory to determine the inactivation potential of any decontaminating approach toward SARS-CoV-2 or any other virus and microorganisms.

5. Conclusions

In summary, we defined 3 kGy as the minimum effective inactivation dose of electron beam radiation for a SARS-CoV-2 titer reduction of more than 4 log units on experimental packaging materials under cold-chain temperatures. Given that the minimum irradiation dose for viral inactivation is far below the upper safe limit for food processing, our study provides a basis for establishing radiation-based sterilization methods for cold-chain food during the current SARS-CoV-2 pandemic.

Data availability

All the data generated during the current study are included in the manuscript.

Ethics statement

This article does not contain any studies with human or animal subjects performed by any of the authors. All experiments involving viruses were performed in biosafety level 3 (BSL-3) facilities, in accordance with the institutional biosafety manual of the Institute of Microbiology, Chinese Academy of Sciences.

Author Contributions

Zihao Wang: investigation, data curation, writing – original draft. Zhentao Liang: conceptualization, methodology. Rongguo Wei: conceptualization, methodology. Hongwei Wang: investigation. Fang Cheng:

investigation. Yang Liu: conceptualization. Songdong Meng: conceptualization, methodology, writing - review&editing, supervision.

Conflicts of Interest

The authors declare that they have no conflict of interest.

Acknowledgments

We are grateful to Prof. Yuhai Bi [Institute of Microbiology, Chinese Academy of Sciences (CAS)] for his technical assistance. We thank Yiping Zhu and all the staff of the biosafety level 3 laboratory at the Institute of Microbiology, CAS, for assistance with the experiments performed. This study was supported by a grant from the Strategic Priority Research Program of the Chinese Academy of Sciences (XDB29040000), the Industrial innovation team grant from Foshan Industrial Technology Research Institute, Chinese Academy of Sciences, the National Natural Science Foundation of China (32070163, 81761128002, 81871297), the China ATOMIC energy authority, Foshan High-level Hospital construction DengFeng plan and Guangdong Province biomedical innovation platform construction project tumor immunobiotherapy.

Appendix A. Supplementary data

Supplementary data to this article can be found online at https://doi.org/10.1016/j.virs.####

References

Al-Hadyan, K., Alsbeih, G., Al-Harbi, N., Judia, S. Bin, Al-Ghamdi, M., Almousa, A., Alsharif, I., Bakheet, R., Al-Romaih, K., Al-Mozaini, M., Al-Ghamdi, S., Moftah, B., Alhmaid, R., 2021. Effect of gamma irradiation on filtering facepiece respirators and SARS-CoV-2 detection. Sci. Rep. 11. https://doi.org/10.1038/s41598-021-99414-6

Bai, C., Zhong, Q., Gao, G.F., 2022. Overview of SARS-CoV-2 genome-encoded proteins. Sci. China Life Sci. 65, 280–294.

Boegel, S.J., Gabriel, M., Sasges, M., Petri, B., D'Agostino, M.R., Zhang, A., Ang, J.C., Miller, M.S., Meunier, S.M., Aucoin, M.G., 2021. Robust Evaluation of Ultraviolet-C Sensitivity for SARS-CoV-2 and Surrogate Coronaviruses. Microbiol. Spectr. 9, 1–10.

Brahmakshatriya, V., Lupiani, B., Brinlee, J.L., Cepeda, M., Pillai, S.D., Reddy, S.M., 2009. Preliminary study for evaluation of avian influenza virus inactivation in contaminated poultry products using electron beam irradiation. Avian Pathol. 38, 245–250.

Chen, C., Feng, Y., Chen, Z., Xia, Y., Zhao, X., Wang, J., Nie, K., Niu, P., Han, J., Xu, W., 2022. SARS-CoV-2 cold-chain transmission: Characteristics, risks, and strategies. J. Med. Virol. 94, 3540–3547.

Chi, Y., Wang, Q., Chen, G., Zheng, S., 2021a. The Long-Term Presence of SARS-CoV-2 on Cold-Chain Food Packaging Surfaces Indicates a New COVID-19 Winter Outbreak: A Mini Review. Front. Public Heal. 9, 1–5.

Chi, Y., Zheng, S., Liu, C., Wang, Q., 2021b. Transmission of SARS-CoV-2 on cold-chain food overpacks: A new challenge. J. Glob. Health 11, 1–4.

Diehl, J.F., 2002. Food irradiation - Past, present and future. Radiat. Phys. Chem. 63, 211–215.

Dziedzic-Goclawska, A., Kaminski, A., Uhrynowska-Tyszkiewicz, I., Stachowicz, W., 2005. Irradiation as a safety procedure in tissue banking. Cell Tissue Bank. 6, 201–219.

Elliott, L.H., McCormick, J.B., Johnson, K.M., 1982. Inactivation of Lassa, Marburg, and Ebola viruses by gamma irradiation. J. Clin. Microbiol. 16, 704–708.

Feng, X.L., Li, B., Lin, H.F., Zheng, H.Y., Tian, R.R., Luo, R.H., Liu, M.Q., Jiang, R. Di, Zheng, Y.T., Shi, Z.L., Bi, Y.H., Yang, X. L, 2021. Stability of SARS-CoV-2 on the Surfaces of Three Meats in the Setting That Simulates the Cold Chain Transportation. Virol. Sin. 36, 1069–1072.

Fisher, D., Reilly, A., Zheng, A.K.E., Cook, A.R., Anderson, D.E., 2020. Seeding of outbreaks of covid-19 by contaminated fresh and frozen food. bioRxiv 2020.08.17.255166; doi: https://doi.org/10.1101/2020.08.17.255166

Gidari, A., Sabbatini, S., Bastianelli, S., Pierucci, S., Busti, C., Bartolini, D., Stabile, A.M., Monari, C., Galli, F., Rende, M., Cruciani, G., Francisci, D., 2021. Sars-cov-2 survival on surfaces and the effect of uv-c light. Viruses 13, 2–9.

Grieb, T., Forng, R.Y., Brown, R., Owolabi, T., Maddox, E., Mcbain, A., Drohan, W.N., Mann, D.M., Burgess, W.H., 2002. Effective use of gamma irradiation for pathogen inactivation of monoclonal antibody preparations. Biologicals 30, 207–216.

Guo, M., Yan, J., Hu, Y., Xu, L., Song, J., Yuan, K., Cheng, X., Ma, S., Liu, J., Wu, X., Liu, L., Rong, S., Wang, D., 2022. Transmission of SARS-CoV-2 on Cold-Chain Food: Precautions Can Effectively Reduce the Risk. Food Environ. Virol. 14, 295–303.

He, X., Liu, X., Li, P., Wang, P., Chen, H., Li, W., Li, B., Liu, T., Ma, J., 2022. A Multi-Stage Green Barrier Strategy for the Control of Global SARS-CoV-2 Transmission via Cold Chain Goods 9, 13–16.

Hume, A.J., Ames, J., Rennick, L.J., Duprex, W.P., Marzi, A., Tonkiss, J., Mühlberger, E., 2016. Inactivation of RNA viruses by gamma irradiation: A study on mitigating factors. Viruses 8, 204.

Inagaki, H., Saito, A., Sugiyama, H., Okabayashi, T., Fujimoto, S., 2020. Rapid inactivation of SARS-CoV-2 with Deep-UV LED irradiation. Emerg. Microbes Infect. 9, 1744–1747.

Jain, R., Sarkale, P., Mali, D., Shete, A., Patil, D., Majumdar, T., Suryawanshi, A., Patil, S., Mohandas, S., Yadav, P., 2021. Inactivation of SARS-CoV-2 by gamma irradiation. Indian J Med Res 153, 196–198.

Jarvis, M.C., 2020. Aerosol Transmission of SARS-CoV-2: Physical Principles and Implications. Front. Public Heal. 8, 1–8.

Jeong, M.I., Lee, E.J., Park, S.Y., Kim, M.R., Park, S.R., Moon, Y., Choi, C., Ha, J.H., Ha, S. Do, 2021. Assessment of human norovirus inhibition in cabbage kimchi by electron beam irradiation using RT-qPCR combined with immunomagnetic separation. J. Food Sci. 86, 505–512.

Kampf, G., Todt, D., Pfaender, S., Steinmann, E., 2020. Persistence of coronaviruses on inanimate surfaces and their inactivation with biocidal agents. J. Hosp. Infect. 104, 246–251.

Korystov Yu N, 1992. Contributions of the direct and indirect effects of ionizing radiation to reproductive cell death. Radiat Res 129, 228–234.

Leslie, R.A., Zhou, S.S., Macinga, D.R., 2021. Inactivation of SARS-CoV-2 by commercially available alcohol-based hand sanitizers. Am. J. Infect. Control 49, 401–402.

Li, F., Wang, J., Liu, Z., Li, N., 2022. Surveillance of SARS-CoV-2 Contamination in Frozen Food-Related Samples — China, July 2020 – July 2021. China CDC Wkly. 4, 465–470.

Liu, P., Yang, M., Zhao, X., Guo, Y., Wang, L., Zhang, J., 2020. Cold-chain transportation in the frozen food industry may have caused a recurrence of COVID-19 cases in destination: Successful isolation of SARS-CoV-2 virus from the imported frozen cod package surface Peipei 2, 199–201.

Liu, W., Guan, W., Zhong, N., 2020. Strategies and Advances in Combating COVID-19 in China 6, 1076–1084.

Loveday, E.K., Hain, K.S., Kochetkova, I., Hedges, J.F., Robison, A., Snyder, D.T., Brumfield, S.K., Young, M.J., Jutila, M.A., Chang, C.B., Taylor, M.P., 2021. Effect of inactivation methods on sars-cov-2 virion protein and structure. Viruses 13, 562.

Ma, H., Wang, Z., Zhao, X., Han, J., Zhang, Y., Wang, H., Chen, C., Wang, J., Jiang, F., Lei, J., Song, J., Jiang, S., Zhu, S., Liu, H., Wang, D., Meng, Y., Mao, N., Wang, Y., Zhu, Z., Chen, Z., Wang, B., Song, Q., Du, H., Yuan, Q., Xia, D., Xia, Z., Liu, P., Wu, Y.A., Feng, Z., Gao, R., Gao, G.F., Xu, W., 2021. Long Distance Transmission of SARS-CoV-2 from Contaminated Cold Chain Products to Humans — Qingdao City, Shandong Province, China, September 2020. China CDC Wkly. 3, 637–644.

Mousavi Khaneghah, A., Hashemi Moosavi, M., Oliveira, C.A.F., Vanin, F., Sant'Ana, A.S., 2020. Electron beam irradiation to reduce the mycotoxin and microbial contaminations of cereal-based products: An overview. Food Chem. Toxicol. 143, 111557.

Näslund, J., Lagerqvist, N., Lundkvist, Å., Evander, M., Ahlm, C., Bucht, G., 2008. Kinetics of Rift Valley Fever Virus in experimentally infected mice using quantitative real-time RT-PCR. J. Virol. Methods 151, 277–282.

Ohshima, H., Iida, Y., Matsuda, A., Kuwabara, M., 1996. Damage Induced by Hydroxyl Radicals Generated in the Hydration Layer of γ-Irradiated Frozen Aqueous solution of DNA. J. Radiat. Res. 37, 199–207.

Pan, Y., Zhang, D., Yang, P., Poon, L.L.M., Wang, Q., 2020. Viral load of SARS-CoV-2. Lancet Infect. Dis. 20, 411–412.

Peña, M., Ampuero, M., Garcés, C., Gaggero, A., García, P., Velasquez, M.S., Luza, R., Alvarez, P., Paredes, F., Acevedo, J., Farfán, M.J., Solari, S., Soto-Rifo, R., Valiente-Echeverría, F., 2020. Performance of SARS-CoV-2 rapid antigen test compared with real-time RT-PCR in asymptomatic individuals. Int J Infect Dis, 107, 201-204

Pillai SD, Shayanfar, S., 2017. Electron beam technology and other irradiation technology applications in the food industry. Top Curr Chem (Cham). 375, 6.

Praveen, C., Dancho, B.A., Kingsley, D.H., Calci, K.R., Meade, G.K., Mena, K.D., Pillai, S.D., 2013. Susceptibility of murine norovirus and hepatitis a virus to electron beam irradiation in oysters and quantifying the reduction in potential infection risks. Appl. Environ. Microbiol. 79, 3796–3801.

Predmore, A., Sanglay, G.C., DiCaprio, E., Li, J., Uribe, R.M., Lee, K., 2015. Electron beam inactivation of Tulane virus on fresh produce, and mechanism of inactivation of human norovirus surrogates by electron beam irradiation. Int. J. Food Microbiol. 198, 28–36.

Preuss, T., Kamstrup, S., Kyvsgaard, N.C., Nansen, P., Miller, A., Lei, J.C., 1997. Comparison of two different methods for inactivation of viruses in serum. Clin. Diagn. Lab. Immunol. 4, 504–508.

Ravindran, R., Jaiswal, A.K., 2019. Wholesomeness and safety aspects of irradiated foods. Food Chem. 285, 363–368.

Ruetalo, N., Businger, R., Schindler, M., 2021. Rapid, dose-dependent and efficient inactivation of surface dried SARS-CoV-2 by 254 nm UV-C irradiation. Euro Surveill. 26, 2001718.

Sellera, F.P., Sabino, C.P., Cabral, F. V., Ribeiro, M.S., 2021. A systematic scoping review of ultraviolet C (UVC) light systems for SARS-CoV-2 inactivation. J. Photochem. Photobiol. 8:100068.

Smolko, E.E., Lombardo, J.H., 2005. Virus inactivation studies using ion beams, electron and gamma irradiation. Nucl. Instruments Methods Phys. Res. Sect. B Beam Interact. with Mater. Atoms 236, 249–253.

Sommer, R., Pribil, W., Appelt, S., Gehringer, P., Eschweiler, H., Leth, H., Cabaj, A., Haider, T., 2001. Inactivation of bacteriophages in water by means of non-ionizing (UV-253.7nm) and ionizing (gamma) radiation: A comparative approach. Water Res. 35, 3109–3116.

Song, Z., Xu, Y., Bao, L., Zhang, L., Yu, P., Qu, Y., Zhu, H., Zhao, W., Han, Y., Qin, C., 2019. From SARS to MERS, thrusting coronaviruses into the spotlight. Viruses 11, 59.

Summers, W.C., Szybalski, W., 1967. Gamma-irradiation of deoxyribonucleic acid in dilute solutions: II. Molecular mechanisms responsible for inactivation of phage, its transfecting DNA, and of bacterial transforming activity. J. Mol. Biol. 26, 227–235.

Takeda, Y., Uchiumi, H., Matsuda, S., Ogawa, H., 2020. Acidic electrolyzed water potently inactivates SARS-CoV-2 depending on the amount of free available chlorine contacting with the virus. Biochem Biophys Res Commun 530, 1–3.

To, K. K., Tsang, O. T., Leung, W. S., Tam, A. R., Wu, T. C., Lung, D. C., Yip, C. C., Cai, J. P., Chan, J. M., Chik, T. S., Lau, D. P., Choi, C. Y., Chen, L. L., Chan, W. M., Chan, K. H., Ip, J. D., Ng, A. C., Poon, R. W., Luo, C. T., Cheng, V. C., Chan, J.F, Hung, I.F.H., Chen, Z., Chen, H., Yuen, K.Y., 2020. Temporal profiles of viral load in posterior oropharyngeal saliva samples and serum antibody responses during infection by SARS-CoV-2: an observational cohort study. Lancet Infect Dis. 20, 565–574.

Uema, M., Yonemitsu, K., Momose, Y., Ishii, Y., Tateda, K., Inoue, T., Asakura, H., 2021. Effect of the photocatalyst under visible light irradiation in SARS-CoV-2 stability on an abiotic surface. Biocontrol Sci. 26, 119–125.

Ulloa, S., Bravo, C., Ramirez, E., Fasce, R., Fernandez, J., 2021. Inactivation of SARS-CoV-2 isolates from lineages B.1.1.7 (Alpha), P.1 (Gamma) and B.1.110 by heating and UV irradiation. J. Virol. Methods 295, 114216.

van Doremalen N, T, B., DH, M., MG, H., A, G., BN, W., A, T., JL, H., NJ, T., SI, G., JO, L.-S., E, de W., VJ, M., 2020. Aerosol and Surface Stability of SARS-CoV-2 as Compared with SARS-CoV-1. N Engl J Med 382, 1564–1567.

Wang, M.Y., Zhao, R., Gao, L.J., Gao, X.F., Wang, D.P., Cao, J.M., 2020. SARS-CoV-2: Structure, Biology, and Structure-Based Therapeutics Development. Front. Cell. Infect. Microbiol. 10, 1–17.

Ward RL., 1980. Mechanisms of poliovirus inactivation by the direct and indirect effects of ionizing radiation. Radiat Res. 83, 330–44.

Widera, M., Mühlemann, B., Corman, V.M., Toptan, T., Beheim-Schwarzbach, J., Kohmer, N., Schneider, J., Berger, A., Veith, T., Pallas, C., Bleicker, T., Goetsch, U., Tesch, J., Gottschalk, R., Jones, T.C., Ciesek, S., Drosten, C., 2021. Surveillance of sars-cov-2 in frankfurt am main from october to december 2020 reveals high viral diversity including spike mutation n501y in b.1.1.70 and b.1.1.7. Microorganisms 9, 1–10.

Zhang, N., Gong, Y., Meng, F., Shi, Y., Wang, J., Mao, P., Xia, C., Bi, Y., Yang, P., Wang, F., 2021. Comparative study on virus shedding patterns in nasopharyngeal and fecal specimens of COVID-19 patients. Sci. China Life Sci. 64, 486–488.

Figure legends

Fig. 1. Workflow of inactivation of viruses using electron beam radiation. **A.** The radiation dose required for the inactivation of SARS-CoV-2 was determined using low-energy electron irradiation (LEEI). **B.** HCoV-OC43 was used as a surrogate for SARS-CoV-2 and treated with both LEEI and high-energy electron irradiation (HEEI) to determine the radiation dose required for the inactivation of the virus in different materials.

Fig. 2. Effect of LEEI on the infectivity of SARS-CoV-2 and HCoV-OC43. Up to 10 µL of clarified viral supernatant of $10^{4.6}$ $TCID_{50}$/mL of SARS-CoV-2 (**A**) or $10^{4.75}$ $TCID_{50}$/mL of HCoV-OC43 (**B**) was placed on stainless steel sheet and exposed to increasing doses of LEEI at 4°C or −20°C, respectively. The stainless steel sheet was washed thoroughly with serum-free DMEM, and the solution containing eluted viruses was tested in duplicates using the $TCID_{50}$ assay. Representative microphotographs (magnification × 100) of Vero E6 (**C**) and BHK-21 (**D**) monolayers 72 h post-infection with SARS-CoV-2 or HCoV-OC43 under treatment with the indicated doses of radiation at −20°C are shown. Complete viral inactivation was determined using three consecutive passages of cell culture supernatants on corresponding cells with no cytopathic effect. The data are the mean of triplicate measurements. The experiments were repeated three times with similar results.

Fig. 3. Effect of the tested materials on HCoV-OC43 inactivation using HEEI. Ten microliters of viral stock containing 10^4–10^5 $TCID_{50}$/mL were placed on different materials at 4°C (**A**) or −20°C (**B**). Virus particles were carefully recovered after the indicated doses of radiation and processed for $TCID_{50}$ assay. Complete viral inactivation was verified using three consecutive passages of cell culture supernatants on corresponding cells with no cytopathic effect. The mean ± SD of triplicate measurements is shown. * $P < 0.05$, ** $P < 0.01$.

Fig. 4. Influence of LEEI on the sensitivity of RT-qPCR assay for SARS-CoV-2 detection. Ten microliters of serially diluted (10-fold) viral samples on stainless steel surfaces were exposed to 2 kGy of radiation or not irradiated, and then the viral particles were recovered. SARS-CoV-2 RNA was extracted and subjected to RT-qPCR assays. At each dilution, the Cq detection threshold and linear relationship between $TCID_{50}$ and Cq values for viral *E* (**A** and **D**), *N* (**B** and **E**), and *ORF1ab* (**C** and **F**) genes are shown. The mean ± SD of triplicate measurements is shown.

Fig. 5. Combination of virus culture and RT-qPCR methods. The SARS-CoV-2 with indicated titers placed on stainless steel surfaces were recovered, and the viral suspensions were incubated with Vero E6 monolayers for 72 h. Viral RNA extracted from the cell supernatants was subjected to RT-qPCR assays of the *E*, *N*, and *ORF1ab* genes. SARS-CoV-2 inactivated using 2 kGy of radiation could not be recovered (**A**). Correlation analysis was performed between viral $TCID_{50}$ and Cq values of the *E* (**B**), *N* (**C**), and *ORF1ab* (**D**) genes. The dashed grey line represents the RT-qPCR limit of detection. The data are the mean of triplicate measurements.

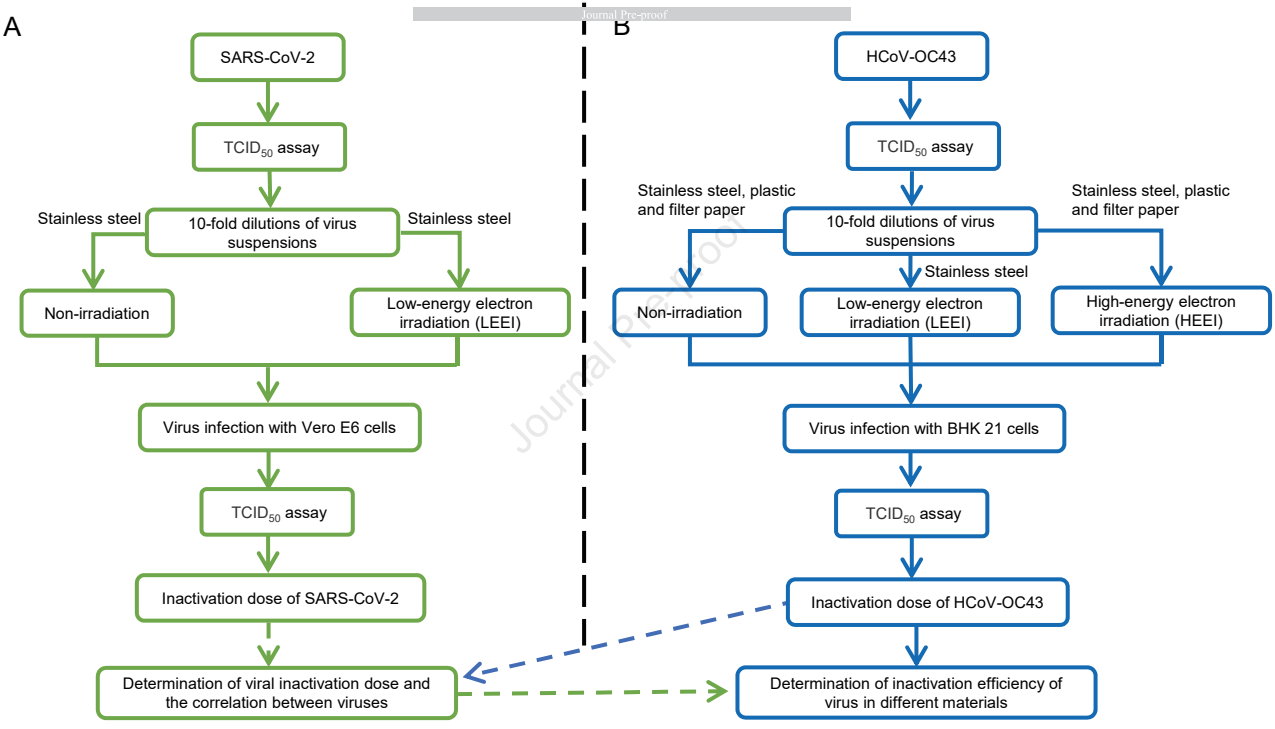

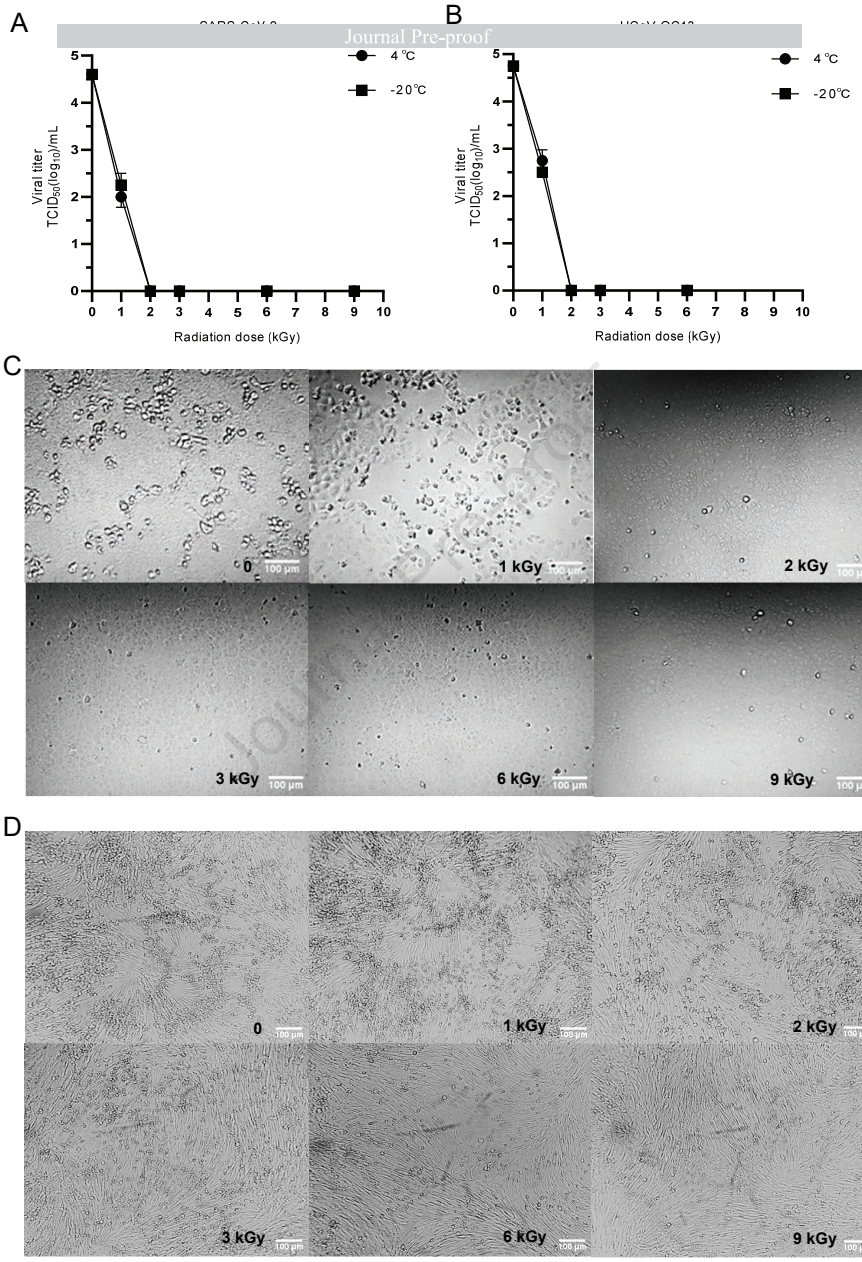

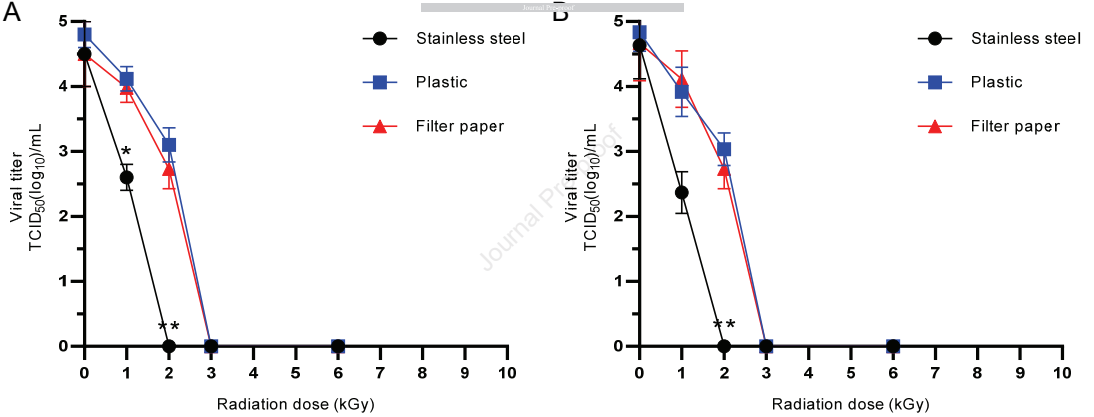
A
B
Stainless steel
Plastic
Filter paper
Viral titer
TCID50(log10)/mL
Radiation dose (kGy)
*
**
0
1
2
3
4
5
6
7
8
9
10

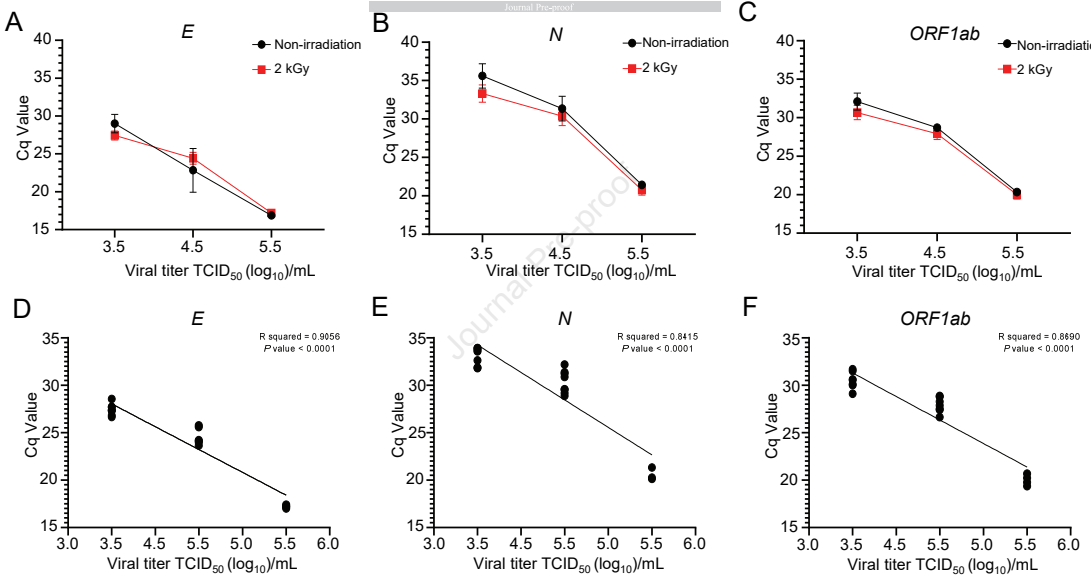

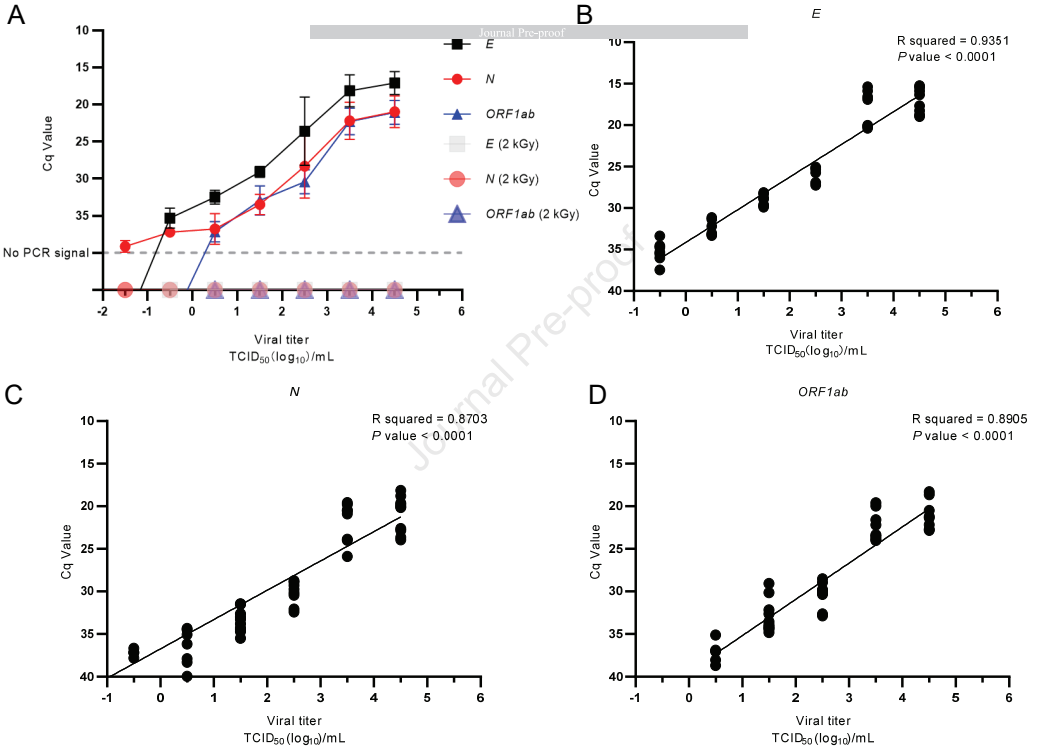

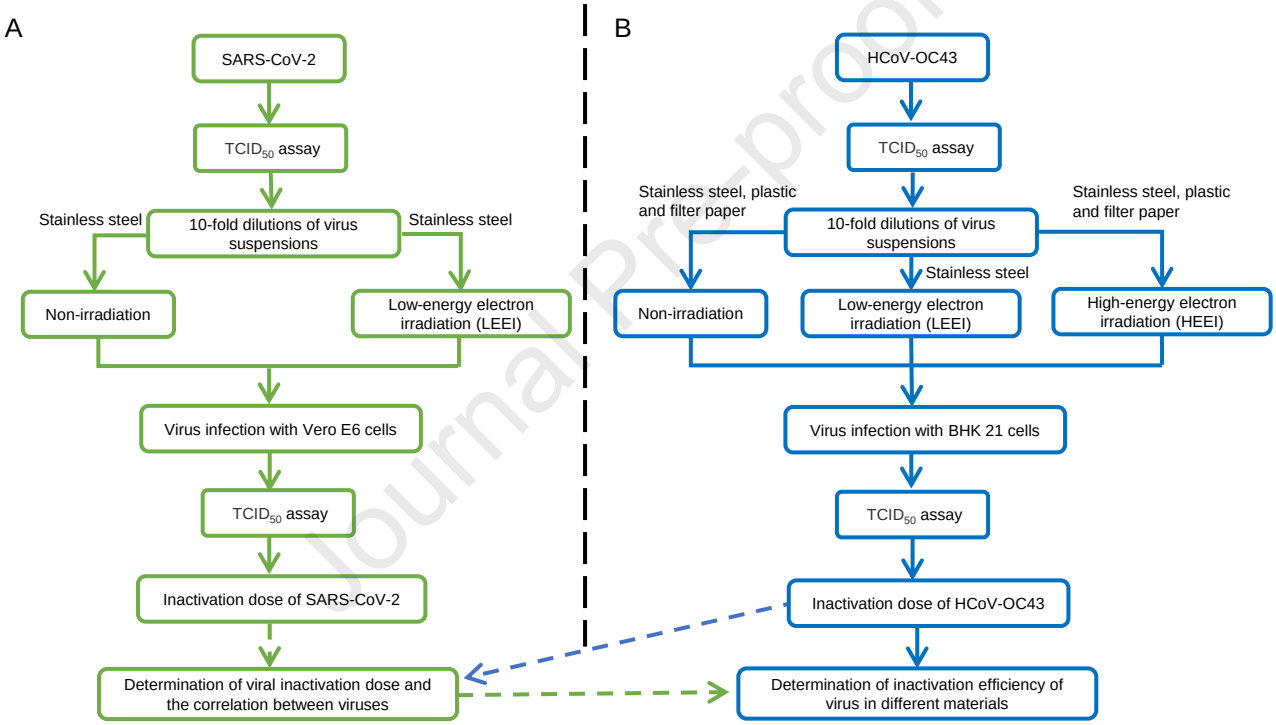

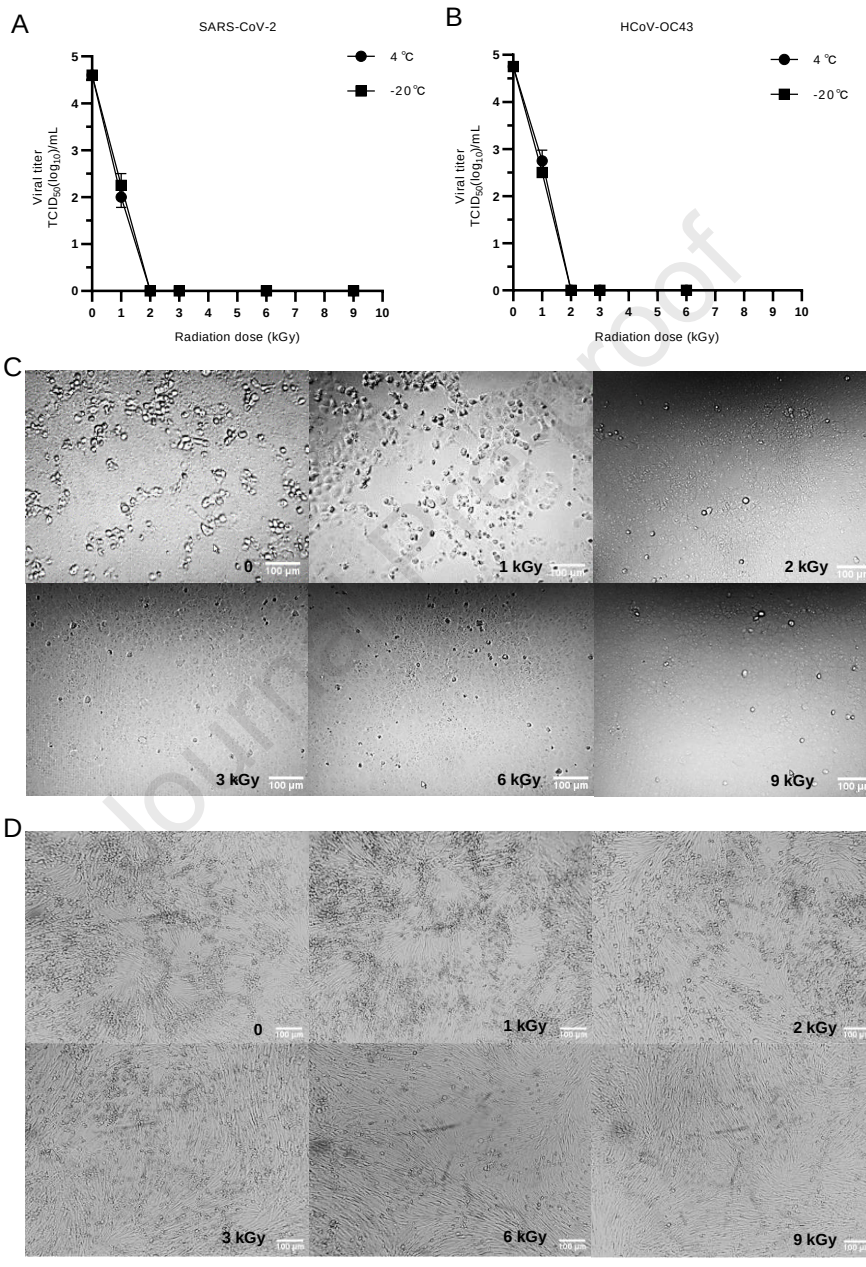
A
SARS-CoV-2
4 ℃
-20℃
Viral titer
TCID50/(log10)/mL
Radiation dose (kGy)
B
HCoV-OC43
4 ℃
-20℃
Viral titer
TCID50/(log10)/mL
Radiation dose (kGy)
C
0
1 kGy
2 kGy
3 kGy
6 kGy
9 kGy
100 μm
D
0
1 kGy
2 kGy
3 kGy
6 kGy
9 kGy